Change in the Microhardness of Composite Ceramics at the CaO−ZrO$_2$/CaO−ZrO$_2$ + Al$_2$O$_3$ Interface

A. A. Dmitrievskiy^{a,} *, D. G. Zhigacheva^a, G. V. Grigoriev^a, and P. N. Ovchinnikov^a

^{a} Derzhavin Tambov State University, Tambov, 392000 Russia
*e-mail: aadmitr@yandex.ru

Two-layer samples of zirconium ceramics stabilized in the tetragonal phase with calcium oxide (C_{CaO} = 6.5 mol %) are obtained by the uniaxial dry pressing of preliminarily prepared mixtures of powders (containing and not containing alumina). The microstructure and mechanical properties (microhardness) near the CaO−ZrO$_2$/CaO−ZrO$_2$ + Al$_2$O$_3$ interface is investigated. An abrupt increase in the microhardness (from 13.7 ± 0.2 GPa to 14.4 ± 0.2 GPa) and Young's modulus (from 195 ± 6 GPa to 210 ± 7 GPa) is revealed when passing from CaO−ZrO$_2$ to CaO−ZrO$_2$ + Al$_2$O$_3$. A high probability of the formation (during sintering) of cracks along the interface of zirconium ceramics, containing and not containing alumina, is demonstrated.

INTRODUCTION

Discovered almost 50 years ago [1], the possibility of the room-temperature stabilization of the tetragonal phase of zirconium dioxide t-ZrO$_2$ (by introducing additives of oxides Y$_2$O$_3$, CeO$_2$, CaO and others), capable of mechanically induced transformation into the monoclinic phase m-ZrO$_2$ (transformation $t \rightarrow m$ provides the transformation-hardening mechanism), significantly increased the strength properties of zirconium ceramics. To date, it has been successfully used for the manufacture of cutting tools, carving guides, cams, seals, valves and pump rings [2]. Due to its biocompatibility, zirconium dioxide has become very popular in biomedical applications [3−5]. In addition, zirconium ceramics are used in the manufacture of solid-oxide fuel cells [6], thermal barriers [7], optical coatings [8], catalysts [9], oxygen sensors [10], and many other devices.

The task of further improving the strength properties of zirconium ceramics is successfully solved by the development of composites based on it. The most popular is zirconium ceramics reinforced with aluminum oxide (ATZ ceramics) [11, 12]. It combines the strengths of zirconium ceramics with those of Al$_2$O$_3$-based ceramics due to manifestation of the dispersion-hardening mechanism [13, 14].

The widest range of problems requiring differences in the bulk and surface properties of structural materials has predetermined the emergence of a new generation of composite materials, i.e., functionally gradient materials [15]. They are multilayer composites in which the composition and properties change continuously or stepwise from one part of the product to another [16]. It is assumed that the simultaneous use of different (including mutually exclusive) properties of components of functionally gradient materials. In this regard, the aim of the work is to study the structure and micromechanical properties of two-layer zirconium ceramics in the area of the interface between parts containing and not containing aluminum oxide.

EXPERIMENTAL

For the manufacture of CaO−ZrO$_2$/CaO−ZrO$_2$ + Al$_2$O$_3$ ceramic samples ZrO$_2$ (Sigma-Aldrich), α-Al$_2$O$_3$ (Hongwu) and CaO (Reachem) powders are used. The molar concentration of the stabilizer (CaO) in relation to ZrO$_2$ (regardless of the presence or absence of Al$_2$O$_3$) remained unchanged: C_{CaO} = 6.5 mol %. In accordance with the previously obtained results [17], the use of calcium oxide (instead of "traditional" yttrium oxide) as a stabilizer of the tetragonal phase of zirconium dioxide makes it possible to significantly increase the resistance of zirconium ceramics to low-temperature degradation. To obtain a composition containing aluminum oxide, to a added 5.8 mol % Al$_2$O$_3$ is added to a CaO−ZrO$_2$ mixture, which, according to [18], provides a high ratio of hardness and fracture toughness of ATZ ceramics.

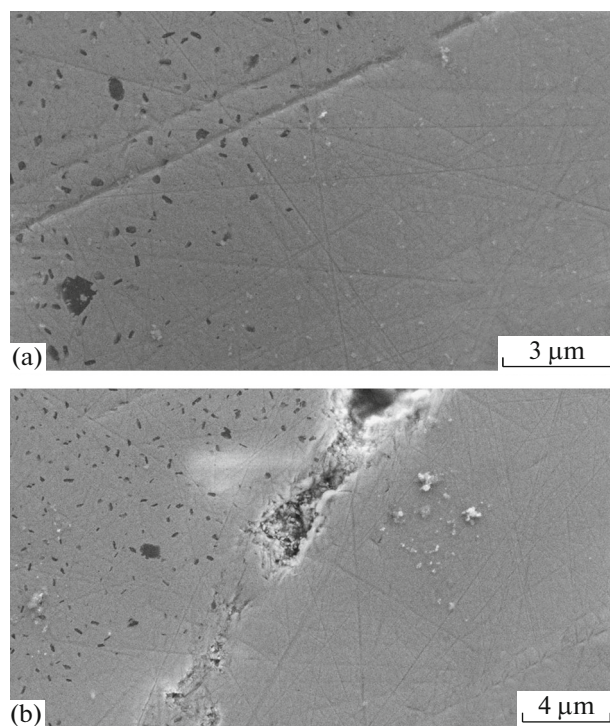The resulting mixtures of powders (containing and not containing aluminum oxide) were dispersed by

Fig. 1. Typical SEM images of the surface areas of the CaO−ZrO$_2$/CaO−ZrO$_2$ + Al$_2$O$_3$ ceramic sample cut far from crack (a) and with a crack along the boundary of the part containing Al$_2$O$_3$ (b).

ultrasound in distilled water (the mass ratio was maintained at 1 : 3). Then, for 5 h, the mixtures were milled in a Pulverisette (Fritsch) planetary mill by ceramic balls made of zirconium dioxide stabilized with yttrium oxide. The ratio of the balls to the ground powder was maintained at 1 : 1. Fine mechanical grinding was carried out with the addition of water (75%) as a grinding medium. This was followed by drying of the mixtures in an oven at a temperature of $T_0 = 80°C$ and normal pressure for 24 hours. The mixtures prepared in this way (containing and not containing Al$_2$O$_3$) were sequentially and in equal amounts poured into a mold. The two-layer samples were molded by uniaxial dry pressing at a load of 500 MPa for 20 min. The samples were sintered in an electric furnace in a two-stage mode (described in detail in [19]) at temperatures of $T_1 = 1300°C$ and $T_2 = 1200°C$. According to [20, 21], a two-stage sintering mode for ceramics based on ZrO$_2$ and Al$_2$O$_3$ ensures the retention of a small grain size (in comparison with single-stage sintering) and a high density of ceramics. The samples obtained had an average crystallite size of ZrO$_2$ and Al$_2$O$_3$ of no more than 100 and 250 nm, respectively. The porosity (measured by the Archimedes method) did not exceed 3%. The samples obtained (in the form of two-layer tablets) were sawn in half, after which the end surface was mechanically ground and polished to measure the microhardness.

The structure of the prepared samples of CaO−ZrO$_2$/CaO−ZrO$_2$+ Al$_2$O$_3$ ceramics was imaged using a Merlin high-resolution scanning electron microscope (SEM) (Carl Zeiss). The microhardness H and Young's modulus E at different distances from the CaO−ZrO$_2$/CaO−ZrO$_2$ + Al$_2$O$_3$ interface were determined using a NanoIndenter G200 device (MTS NanoInstruments). As an indenter, we took the Berkovich pyramid, the penetration depth of which did not exceed 6 microns.

RESULTS AND DISCUSSION

Figure 1a shows a typical SEM image of a section of the sample cut surface of CaO−ZrO$_2$/CaO−ZrO$_2$ + Al$_2$O$_3$ ceramics. According to a large number of published data and elemental mapping of the surface areas of samples with a similar composition, performed in [22], dark spots in the presented SEM image are identified as Al$_2$O$_3$. It can be seen that alumina crystallites are uniformly distributed in one part of the sample (top left) and are absent in the other part (bottom right). This gives grounds to assert that in the prepared samples there is a sharp boundary between the parts containing and not containing Al$_2$O$_3$ crystallites. More detailed analysis of the SEM images did not reveal any other signs of differences between these parts (the average size of ZrO$_2$ crystallites, the presence of pores and other signs).

It is important to note that almost every sample contains cracks that extend strictly along the CaO−ZrO/CaO−ZrO$_2$ + Al$_2$O$_3$ ceramic interface (Fig. 1b). Cracking occurs during the sintering process. The most probable cause of the observed cracking is a difference in the temperature coefficients of linear expansion of zirconium and corundum ceramics [23] and, as a consequence, the parts of the studied samples containing and not containing Al$_2$O$_3$.

I was carried out in areas of the polished surface at least 500 μm away from the cracks. The side of the imprint of the indenter (Berkovich pyramid) did not exceed 45 μm. We note that the grooves observed in the SEM images are traces of mechanical polishing, have a small (compared to the indentation of the indenter) size and do not have a noticeable effect on the determined value of the microhardness. Strict control of the spatial arrangement of the indentations of the indenter made it possible to plot the dependences of the microhardness H and Young's modulus E of the material from distance d to the CaO−ZrO$_2$/CaO−ZrO$_2$ + Al$_2$O$_3$ ceramic interface (Fig. 2).

From the presented dependences it can be seen that in the immediate vicinity of the interface there is an abrupt change in the values H and E. At distances d exceeding 100 μm from the interface (twice the side of the indentation of the indenter), the dependence $H(d)$ and $E(d)$ become saturated. The microhardness and Young's modulus take on values characteristic of the
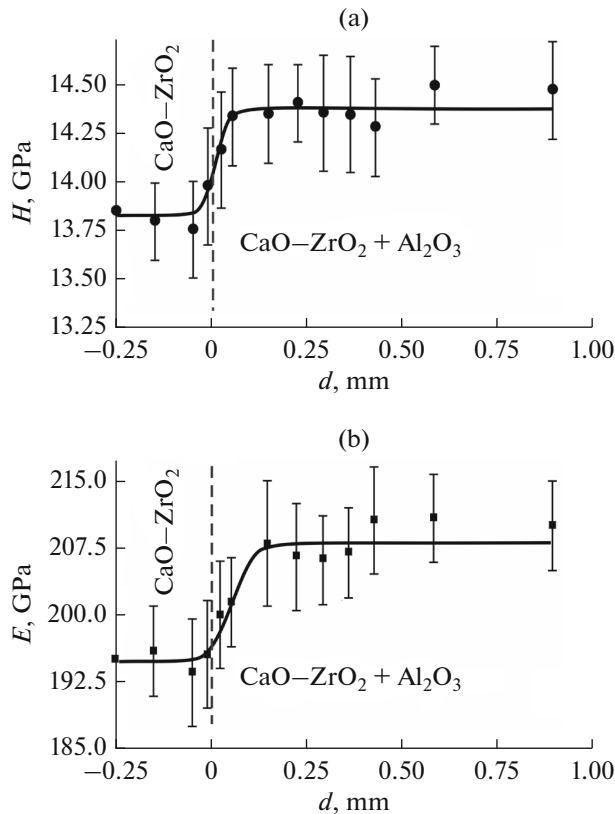
Fig. 2. Dependences of the microhardness H (a) and Young's modulus E (b) on the distance d to the interface between parts of the sample of zirconium ceramics, containing and not containing Al_2O_3.

corresponding ceramics $CaO-ZrO_2$ and $CaO-ZrO_2 + Al_2O_3$.

CONCLUSIONS

The possibility of manufacturing (by the method of uniaxial dry pressing followed by two-stage sintering) zirconium ceramics with a sharp interface between the compositions $CaO-ZrO_2/CaO-ZrO_2 + Al_2O_3$ is shown. In the immediate vicinity of the interface (~100 microns) there is an abrupt change in the microhardness and Young's modulus from the values typical for $CaO-ZrO_2$ ($H = 13.7 \pm 0.2$ GPa, $E = 195 \pm 6$ GPa) to values typical for ceramics $CaO-ZrO_2 + Al_2O_3$ ($H = 14.4 \pm 0.2$ GPa, $E = 210 \pm 7$ GPa). The result obtained can be used in the development of articles made of composite ceramics based on zirconium dioxide, the bulk and surface mechanical properties of which must meet various requirements.

A disadvantage of the proposed method is the high probability of cracking (caused by a difference in the temperature coefficients of the linear expansion of ZrO_2 and Al_2O_3) at the interface between ceramics containing and not containing aluminum oxide. The development of ways to implement the ideology of functionally gradient materials, i.e., the formation of a smooth transition from $CaO-ZrO_2$ to $CaO-ZrO_2 + Al_2O_3$, will ensure preservation of the integrity of composite ceramics during sintering and will be the subject of future research.

CONFLICT OF INTEREST

We declare that we have no conflicts of interest.

REFERENCES

1. R. C. Garvie, R. H. J. Hannink, and R. T. Pascoe, Nature **258**, 703 (1975).
https://doi.org/10.1038/258703a0

2. X. Zhang, X. Wu, and J. Shi, J. Mater. Res. Technol. **9**, 9029 (2020).
https://doi.org/10.1016/j.jmrt.2020.05.131

3. Y. Akagawa, Y. Ichikawa, H. Nikai, and H. Tsuru, J. Prosthet. Dent. **69**, 599 (1993).
https://doi.org/10.1016/0022-3913(93)90289-z

4. H. Shin, H. Ko, and M. Kim, Restor. Dent. Endod. **41**, 167 (2016).
https://doi.org/10.5395/rde.2016.41.3.167

5. R. Galante, C. G. Figueiredo-Pina, and A. P. Serro, Dent. Mater. **35**, 825 (2019).
https://doi.org/10.1016/j.dental.2019.02.026

6. N. Mahato, A. Gupta, and K. Balani, Nanomater. Energy **1**, 27 (2012).
https://doi.org/10.1680/nme.11.00004

7. J. F. Shackelford and R. H. Doremus, in *Ceramic and Glass Materials: Structure, Properties and Processing* (Springer, Berlin, 2008), p. 169.

8. V. Thakare, Int. J. Eng. Res. Dev. **5**, 25 (2012).
http://www.ijerd.com/paper/vol5-issue1/F05012528.pdf.

9. E. Krumov, J. Dikova, K. Starbova, D. Popov, V. Blaskov, K. Kolev, and L. D. Laude, J. Mater. Sci.: Mater. Electron. **14**, 759 (2003).
https://doi.org/10.1023/A:1026176431171.pdf

10. J. H. Lee, J. Mater. Sci. **38**, 4247 (2003).
https://doi.org/10.1023/A:1026366628297.pdf

11. G. Soon, B. Pingguan-Murphy, K. W. Lai, and S. A. Akbar, Ceram. Int. **4**, 12543 (2016).
https://doi.org/10.1016/j.ceramint.2016.05.077

12. A. Maji and G. Choubey, Mater. Today Proc. **5**, 7457 (2018).
https://doi.org/10.1016/j.matpr.2017.11.4l7

13. F. Zhang, L. F. Lin, and E. Z. Wang, Ceram. Int. **41**, 24l7 (2015).
https://doi.org/10.1016/j.ceramint.2015.06.081

14. J.-K. Lee, M. J. Kim, and E. G. Lee, J. Mater. Sci. Lett. **21**, 259 (2002).
https://doi.org/10.1023/A:1014737614591

15. D. V. Min'ko, K. E. Belyavin, and V. K. Sheleg, *Theory and Practice of Obtaining Functionally Graded Materials* (Beloruss. Natl. Tekh. Univ., Minsk, 2020) [in Russian].

16. E. M. M. Ewais, D. H. A. Besisa, Z. I. Zaki, and A. E. H. T. Kandil, J. Eur. Ceram. Soc. **32**, 1561 (2012).
https://doi.org/10.1016/j.jeurceramsoc.2012.01.016

17. A. A. Dmitrievskiy, D. G. Zhigacheva, N. Yu. Efremova, and A. V. Umrikhin, Nanotechnol. Russ. **14**, 125 (2019). https://doi.org/ doi
https://doi.org/10.1134/S1995078019020058

18. A. A. Dmitrievskii, A. O. Zhigachev, D. G. Zhigacheva, and A. I. Tyurin, Tech. Phys. **64**, 86 (2019).
https://doi.org/ doi
https://doi.org/10.1134/S1063784219010092

19. A. A. Dmitrievskii, A. I. Tyurin, A. O. Zhigachev, D. G. Guseva, and P. N. Ovchinnikov, Thech. Phys. Lett. **44**, 141 (2018). https://doi.org/ doi
https://doi.org/10.1134/S1063785018020219

20. J. Binner, K. Annapoorani, A. Paul, and I. Santacruz, J. Eur. Ceram. Soc. **28**, 973 (2008).
https://doi.org/10.1016/j.jeurceramsoc.2007.09.002

21. D. Galusek, K. Ghillanyova, J. Sedlacek, and J. Kozankova, J. Eur. Ceram. Soc. **32**, 1965 (2012).
https://doi.org/10.1016/j.jeurceramsoc.2011.11.038

22. A. A. Dmitrievskii, A. O. Zhigachev, D. G. Zhigacheva, and V. V. Rodaev, Tech. Phys. **65**, 2016 (2020).
https://doi.org/10.1134/S1063784220120075

23. Yu. I. Komolikov, I. D. Kashcheev, and V. R. Khrustov, Refract. Ind. Ceram. **57**, 516 (2017).
https://doi.org/10.1007/s11148-017-0015-1